



# The use of cardiovascular magnetic resonance as an early non-invasive biomarker for cardiotoxicity in cardio-oncology

Matthew K. Burrage, Vanessa M. Ferreira

Oxford Centre for Clinical Magnetic Resonance Research (OCMR), Division of Cardiovascular Medicine, Radcliffe Department of Medicine, University of Oxford, Oxford, UK

*Contributions:* (I) Conception and design: All authors; (II) Administrative support: None; (III) Provision of study materials or patients: None; (IV) Collection and assembly of data: None; (V) Data analysis and interpretation: None; (VI) Manuscript writing: All authors; (VII) Final approval of manuscript: All authors.

*Correspondence to:* Professor Vanessa Ferreira. Associate Professor of Cardiovascular Medicine, University of Oxford Centre for Clinical Magnetic Resonance Research (OCMR), Level 0 John Radcliffe Hospital, Oxford, OX3 9DU, UK. Email: [vanessa.ferreira@cardiov.ox.ac.uk](mailto:vanessa.ferreira@cardiov.ox.ac.uk).

**Abstract:** Contemporary cancer therapy has resulted in significant survival gains for patients. However, many current and emerging cancer therapies have an associated risk of cardiotoxicity, either acutely or later in life. Regular cardiac screening and surveillance is recommended for patients undergoing treatment for cancer, with emphasis on the early detection of cardiotoxicity before irreversible complications develop. Cardiovascular magnetic resonance imaging is able to accurately assess cardiac structure, function, and perform advanced myocardial tissue characterisation, including perfusion, features which may facilitate the diagnosis and management of cardiotoxicity in cancer survivors. This review outlines the current standards for the diagnosis and screening of cardiotoxicity, with particular focus on current and future applications of cardiovascular magnetic resonance imaging.

**Keywords:** Cardiovascular magnetic resonance (CMR); cardio-oncology; cardiotoxicity

Submitted Feb 05, 2020. Accepted for publication May 07, 2020.

doi: 10.21037/cdt-20-165

View this article at: <http://dx.doi.org/10.21037/cdt-20-165>

## Introduction

Remarkable advancements in the treatment of cancer has led to significantly improved long-term survival for many cancer patients. However, cardiovascular disease is a leading cause of morbidity and mortality in cancer survivors, due in part to the well-documented late cardiotoxic effects of specific cancer therapies (1-4). The risk of late cardiovascular disease, compounded by the development or progression of age-related cardiovascular risk factors, may attenuate many of the survival gains from contemporary cancer treatment (5). Cardio-oncology is a rapidly emerging field focused on the assessment of cardiovascular disease in patients with cancer and cancer survivors (6). Most focus has been on the early detection of cardiotoxicity and predicting future cardiac dysfunction, although multiple other manifestations of

cardiotoxicity may occur (7,8) (Table 1).

Cancer therapy-related cardiac dysfunction (CTRCD) is one of the most serious consequences of cardiotoxic therapy, and has historically been associated with a worse prognosis compared with other forms of heart failure (9). This is particularly true when clinical presentation is late after cancer therapy, at which stage myocardial injury is more likely to be permanent and heart failure more resistant or refractory to standard treatment (10). Early detection of cardiotoxicity is thus crucial and presents opportunity for personalised risk-stratification and early therapeutic intervention before irreversible heart failure occurs. This review will focus on the current state of play for the diagnosis and screening of cardiotoxicity, with particular focus on current and future applications of cardiovascular

**Table 1** Cardiovascular complications of cancer therapy

Myocardial dysfunction and heart failure
Coronary artery disease
Valvular heart disease
Arrhythmias
Arterial hypertension
Thromboembolic disease
Peripheral vascular disease and stroke
Pulmonary hypertension
Pericardial complications

Modified from Zamorano *et al.* (8).

magnetic resonance (CMR) imaging.

### Non-invasive imaging in cardio-oncology

The key principle behind imaging in cardio-oncology is the early detection of cardiotoxicity, which may allow early intervention to minimise or prevent irreversible damage, rather than late detection and subsequent need for rescue therapies. This may be achieved via several complementary approaches (11):

- (I) Baseline cardiovascular risk assessment (to identify those individuals with pre-existing cardiovascular disease or multiple risk factors who are at higher risk of cardiotoxicity).
- (II) Cardiac monitoring during cancer therapy to detect early cardiovascular injury (with the option of cardioprotective therapeutic strategies) and predicting the likelihood of recovery.
- (III) Detecting cardiovascular injury in long-term cancer survivors via routine surveillance.

### Echocardiography

Currently, central to these approaches is the use of transthoracic echocardiography (TTE), which has supplanted radionuclide multiple-gated acquisition scans as the initial non-invasive imaging modality of choice for assessments of cardiac function. TTE can screen patients for cardiotoxicity risk factors [such as pre-existing left ventricular (LV) dysfunction, significant valvular abnormalities, underlying cardiomyopathies, or regional wall motion abnormalities which may indicate coronary artery disease] and is a

cheap, widely available tool that is well-suited to ongoing monitoring. Current consensus recommendations support screening and surveillance with echocardiography for all patients at increased cardiovascular risk, given that most definitions of cardiotoxicity are based on a quantitative decline in left ventricular ejection fraction (LVEF) from pre-treatment values (12). There remains some variation in the definition of CTRCD between different society guidelines, likely reflecting the diversity of cancer treatments and their impact on cardiac function (*Table 2*) (13). Generally, a >5–10 percentage point decrease in LVEF to a value below the lower limit of normal is accepted to support a diagnosis of cardiotoxicity, with further criteria dependent on symptom status.

Traditionally, LVEF calculated by the two-dimensional (2D) TTE Simpson's biplane method is the most widely used parameter to evaluate cardiac function. The main limitation of serial assessment of LVEF on 2D-TTE is its relatively moderate reproducibility, which raises concerns about erroneously stopping cancer therapy due to LVEF changes that may have only occurred due to measurement variability (14). One comparative study reported an overall mean difference of  $-0.3\% \pm 6.1\%$  for repeat measurement of ejection fraction using 2D-TTE, with a coefficient of variability (CoV) of 11.5% (15). Three-dimensional (3D) TTE does not rely on geometric assumptions of the LV and is the most reproducible echocardiographic technique for serial LVEF and LV volume assessments, but is dependent on image quality, acoustic windows, availability, and operator experience (14). One study found that 3D-TTE was feasible in only 66% of patients post-anthracycline chemotherapy for breast cancer, due to poor echocardiographic windows (16). Contrast echocardiography may also be used to improve endocardial border definition in patients with suboptimal image quality.

There has been increasing interest in the early detection of subclinical cardiotoxicity, as this may represent an opportunity to prevent or reverse its progression with prompt initiation of cardioprotective heart failure therapies (12,17), and the opportunity to develop potential new CTRCD-targeted therapies. This represents a shift towards newer markers of subclinical cardiac dysfunction, as it is increasingly recognised that many cancer therapies may induce processes that do not result in an early change in LVEF (18–20). Although a strong predictor of cardiac outcomes, LVEF lacks sensitivity for detecting subtle changes in cardiac function due to early myocellular damage (12,21). Even patients with high-grade myocellular injury

**Table 2** Definitions of cardiotoxicity

Organisation	Definition of cardiotoxicity	Comments
ASE/EACVI	LVEF fall by >10% to absolute EF <53%	Change in LV function may be global or regional Symptomatic or asymptomatic for heart failure
ESC	LVEF fall by >10% from baseline to EF <50%	Symptomatic or asymptomatic for heart failure
NCI	CTCAE Heart Failure Grade 1–5	Grade 1 (asymptomatic) Grade 2 (mild to moderate symptoms) Grade 3 (symptomatic on minimal exertion/at rest) Grade 4 (life-threatening) Grade 5 (death)
CCS	LVEF fall by >10% from baseline or LVEF <53%	Guidelines also recommend (I) 3D echocardiography or same imaging modality during cancer therapy, (II) myocardial strain imaging and (III) cardiac biomarkers (N-terminal pro brain natriuretic peptide, troponin) for early detection
ESMO	Symptomatic decline in LVEF of at least 5% to <55% or asymptomatic decline in LVEF of at least 10% to <55%	Symptoms for congestive heart failure with signs including but not limited to S3 gallop, tachycardia, or both  Decline in LVEF either global or more severe in the septum

ASE, American Society of Echocardiography; CCS, Canadian Cardiovascular Society; CTCAE, Common Terminology Criteria for Adverse Events; EACVI, European Association of Cardiovascular Imaging; EF, ejection fraction; ESC, European Society of Cardiology; ESMO, European Society of Medical Oncology; LV, left ventricular; NCI, National Cancer Institute; reproduced from Chung *et al.* (13).

on biopsy may not display a significant change in LVEF (22). Myocardial deformation indices, such as global longitudinal strain (GLS) on 2D-TTE, have shown significant promise in the detection of subclinical cardiotoxicity; it was indeed the strongest predictor of CTRCD during treatment, and has now been incorporated into current consensus statements (8,23-25). A relative percentage decrease in GLS of >15% from baseline is very likely to be of clinical significance (23,26). The ongoing SUCCOUR trial is the first randomised controlled study to base treatment decisions on GLS, and will inform guidelines on the role of GLS in surveillance for CTRCD (27). It is important to note, however, that GLS measurements may be subject to inter-vendor variability, with up to 3.7% strain units absolute difference between vendors seen in one comparison study (28).

Current expert consensus recommends a baseline echocardiogram for the calculation of LVEF (using 3D-TTE and GLS measurements where available) to determine an individual's risk at commencement of cancer-therapy, as well as for ongoing monitoring during

treatment and beyond (26). If the LVEF is <53%, or if poor image quality prevents accurate assessment, then CMR is recommended (20).

### Cardiovascular magnetic resonance

Although initially only reserved for cardiac assessment in patients with suboptimal TTE images, mainly due to previous limited availability and cost concerns, CMR is now an established cardiac imaging modality, both in the clinical and research spheres, as a comprehensive 'one-stop-shop' for cardiovascular assessment, and increasingly used to assess for cardiotoxicity (*Figure 1*).

CMR is highly accurate in assessing cardiac structure and function, and is the gold-standard for accurate serial evaluation of cardiac volumes and function with high reproducibility (15). A comparative study of CMR and 2D-TTE for serial assessment of LVEF showed an overall absolute mean difference of  $0.7\% \pm 2.2\%$  (CoV 3.2%) for CMR compared with  $-0.3\% \pm 6.1\%$  (CoV 11.5%) for 2D-TTE (15). CMR is thus superior to echocardiography

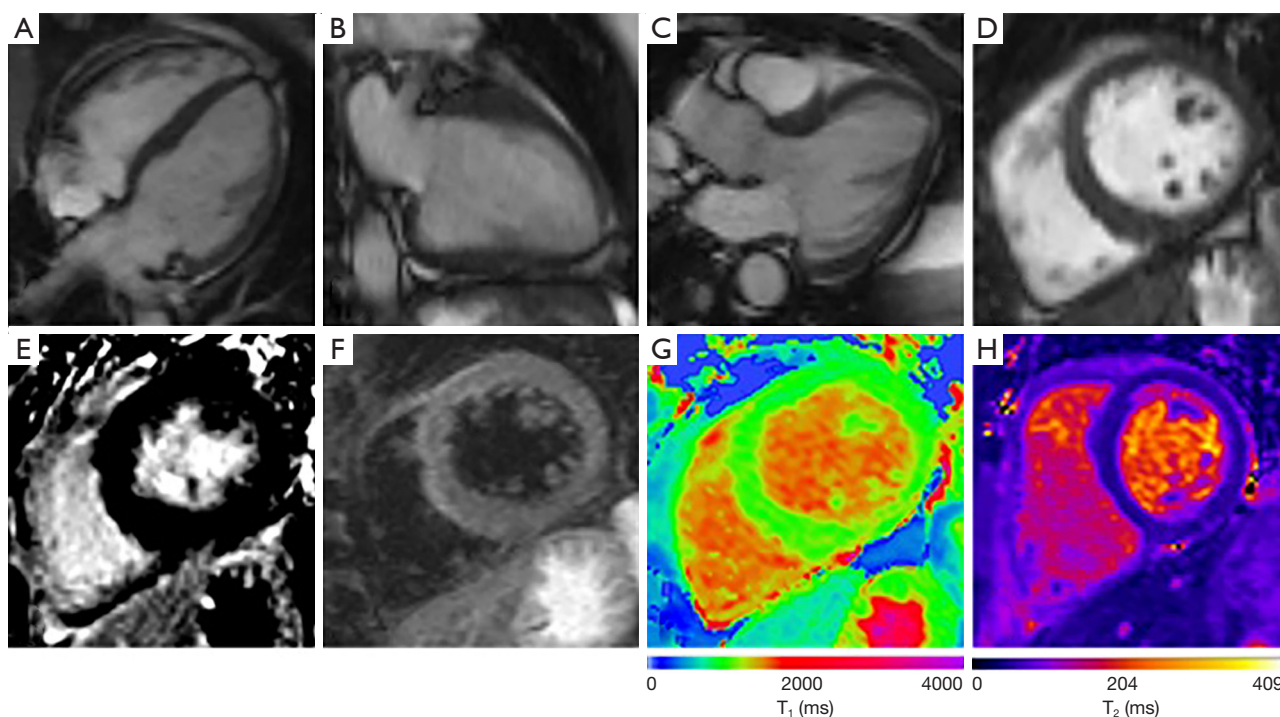


**Figure 1** CMR techniques for assessment of cardiotoxicity. Different CMR techniques available for the assessment of cardiotoxicity including cine imaging in the horizontal long-axis (A), vertical long-axis (B), left ventricular outflow tract (C) views, used for anatomical assessment, while quantification of cardiac volumes is performed using a short-axis (D) stack. Tissue characterisation techniques include late gadolinium imaging (E), T2-weighted imaging (F), and parametric T1- (G) and T2-mapping (H).

in this regard, particularly for detecting subclinical declines in LVEF early after cardiotoxic therapy (29-31). One study reported that 2D-TTE overestimated mean LVEF by 5%, with 11% of patients misclassified as having LVEFs >50% (i.e., above the threshold for the diagnosis of CTRCD) (32). Even when applying 3D-TTE techniques, which demonstrated less variability, the investigators concluded that these methodology lacked the desired accuracy to reliably identify subtle 5% changes in LVEF that may have major management implications (32).

CMR is able to image any desired plane without acoustic window limitations. A contiguous short-axis stack of ventricular slices with high spatial resolution is acquired from the base to the apex of the heart using steady-state free precession cine imaging. Image analysis by contouring the endocardial borders of the short-axis views at end-diastole and end-systole allows calculation of the LV mass, LV end-diastolic volume (LVEDV), LV end-systolic volume (LVESV), stroke volume and LVEF (33). A similar approach is routinely used to provide accurate right ventricular volumes and systolic function. Accurate and reproducible

determination of cardiac volumes is particularly important for reliable serial assessments of cardiac function.

Myocardial deformation indices (such as systolic and diastolic strain and strain rate) may also be derived using several different CMR imaging techniques (34). The most widely used is CMR tissue tagging, which magnetically labels or tags different myocardial regions in standard long- and short-axis cines using non-selective saturation pulses (35). These tags follow the myocardium during contraction, allowing direct measurement of myocardial deformation. Although tagging is considered the reference standard for strain quantification, it requires dedicated acquisition sequences and time-consuming image post-processing (36). More recently, CMR feature tracking (CMR-FT) has been applied to standard long- and short-axis cine images as a newer and simpler technique for estimating strain using a block-matching approach (36). Myocardial boundaries are identified, with regions of interest tracked along the cardiac cycle during post-processing to compute strain indices from both long- and short-axis cines. CMR-FT has reasonable agreement with myocardial tagging for global strain indices (37,38).

Similar to echocardiography, these estimates of local myocardial wall strain and torsion in three-dimensions (longitudinal, radial and circumferential) can detect mild or subclinical changes in cardiac function. Global longitudinal strain (GLS) is derived from horizontal long-axis (HLA) and vertical long-axis (VLA) cines, while global circumferential strain (GCS) is derived from short-axis cines. GLS on feature-tracking CMR may identify early LV dysfunction and has been shown to independently predict all-cause mortality in patients with ischaemic and non-ischaemic cardiomyopathy (39). GCS and GLS on CMR have both been shown to correlate strongly with subclinical LVEF declines and increases in LVEDV following cardiotoxic therapy (40–42). Global strain values are more robust and reproducible than regional ones, with GLS and GCS being the most consistent (34). Of the CMR-derived strain values, GCS has the best interobserver agreement and inter-study reproducibility [CoV 20.3%; interclass correlation coefficient (ICC) 0.7], while global radial strain (GRS) has the worst (CoV 33.3%; ICC 0.44) (43). Currently, most CMR strain measures are not done routinely, and mostly performed in a research capacity, subject to similar post-processing vendor limitations as echocardiography. One study of intervender reproducibility (TomTec, Unterschleissheim, Germany and Circle, CVI42, Calgary, Canada) showed significant differences of up to 4.8% in GCS between vendors, despite GCS being the most reproducible global strain parameter with the lowest intra- and interobserver variability (when assessed with TomTec) (44). Further work and standardisation are needed before these can be applied more widely in the clinical setting.

## CMR tissue characterisation techniques

### *Late gadolinium enhancement (LGE) imaging*

One of the strengths of CMR is its ability to perform non-invasive advanced myocardial tissue characterisation. Late gadolinium enhancement (LGE) imaging was the prototypal CMR tissue characterisation technique, allowing the differentiation of ischaemic heart disease from non-ischaemic cardiomyopathies via characteristic enhancement patterns (45). LGE imaging is based on the extravascular-extracellular (EV-EC) distribution of gadolinium-based contrast agents (GBCAs). It exploits the differences in GBCA wash-in (transfer from the intravascular to EV-EC space after bolus injection) and washout (renal clearance) kinetics in normal and fibrotic myocardium. This allows the visual differentiation of normal from affected myocardium,

based on the image brightness arising from differences in the distribution of GBCA (46).

LGE images are acquired using an inversion-recovery T1-weighted (T1W) sequence, following intravenous GBCA administration. The inversion time is adjusted so that normal myocardium signal is nulled to appear black on LGE images; prolonged accumulation of GBCA and delayed washout in scarred/fibrotic myocardium would cause these areas to appear white on LGE images. Images are typically acquired to allow full anatomical assessment of the ventricular myocardium with long-axis and short-axis views covering the LV. Areas of increased GBCA uptake are best appreciated approximately 10–20 minutes after contrast injection. Technical considerations include the choice of optimal inversion time (TI) for nulling of the normal myocardium, the amount and type of contrast agent used, and the time taken between injection and image acquisition, in view of myocardial blood flow against renal clear-out efficacy (47).

LGE imaging is an excellent discriminator for areas of focal scarring/fibrosis; subendocardial or transmural enhancement is classically seen in myocardial infarction, while midwall and subepicardial enhancement may be seen in non-ischaemic cardiomyopathies or myocarditis. However, one of the inherent limitations of LGE, is its reliance on areas of presumed normal myocardium for nulling, which is required to highlight areas of pathology. Thus, detection of diffuse pathology, like diffuse myocardial fibrosis, is challenging. Further, LGE lacks the ability to differentiate active from chronic lesions, and is not designed to image myocardial oedema or inflammation, but there are other CMR tissue characterisation techniques able to address this.

### *T2-weighted (T2W) imaging*

T2W imaging techniques are conventionally used to identify areas of myocardial oedema and inflammation. Dark-blood and bright-blood T2W imaging methods are available. Areas of increased myocardial water content are detected as high signal on T2W imaging. This may be assessed semi-quantitatively by comparing the myocardium T2 signal intensity (SI) to a reference region of interest (ROI), either in unaffected myocardium or outside the myocardium in skeletal muscle, and calculating the T2 SI ratio. However, this technique may be limited by the need for a reference ROI in an area of presumed normal tissue, which may not exist in global myocardial inflammation,

and in cases of reference skeletal muscle involvement from systemic inflammatory processes (48). New fully-quantitative pixel-wise T1- and T2-mapping techniques circumvent many of the limitations of these conventional CMR tissue characterisation techniques.

### *Parametric (T1-, ECV, and T2-) mapping*

Parametric T1- and T2-mapping techniques allow more advanced tissue characterisation via directly quantitative pixel-by-pixel maps, without the need for reference ROIs in presumed normal tissue. Detailed review of the technical aspects and MR physics principles may be found in the most recent Society for Cardiovascular Magnetic Resonance (SCMR) Mapping Consensus Statement 2017 (49).

Briefly, T1 is the longitudinal (or spin-lattice) relaxation time of a tissue. Native (pre-contrast) T1 values reflect signal from both the intra- and extra-cellular myocardial compartments. Each tissue type exhibits a specific range of normal T1 values, deviation from which may indicate pathology or a change in physiology (49). Native T1 relaxation times are sensitive to increased tissue free water content. Native T1 is prolonged by myocardial inflammation and oedema, as well as areas of expanded extracellular space, such as in focal and diffuse fibrosis. On the other hand, native T1 relaxation time is typically shortened by iron, fat, and gadolinium-based contrast agents (50). There is increasing interest to quantify the myocardial extracellular volume (ECV), which may be estimated non-invasively using pre- and post-contrast myocardial and blood T1 values, adjusted for blood haematocrit. An increased ECV may act as a surrogate marker for diffuse interstitial fibrosis when other confounding factors of an expanded extracellular space (such as myocardial oedema and amyloidosis) have been ruled out.

T2, or the transverse (spin-spin) relaxation time, is the time constant governing the exponential decay of transverse magnetization. Similar to T1 values, T2 values reflect global signal from the intra- and extra-cellular myocardial compartments, with each tissue type having an established normal range of T2 values, depending on the T2-mapping method used. Increased T2 values generally reflect increased tissue free water content and are used to detect myocardial inflammation and oedema.

Multiple CMR T1 and T2 mapping techniques exist, each with their own metrological properties, normal ranges and degree of clinical validation. It is currently recommended to establish a local normal range,

benchmarked against published norms for the method used where available, given the sensitivity of T1 and T2 values to the method, hardware and software platforms used to measure them; standardised methods and protocols are still being established (49).

Parametric pixel-wise T1- and T2-mapping have shown particular utility in detecting subtle myocardial inflammatory changes in the early stages of disease, and have been validated in a variety of systemic conditions, including the diagnosis of myocarditis (51-54). Additionally, measurement of ECV has also shown significant promise as a surrogate marker for diffuse myocardial fibrosis, overcoming the limitations of LGE in this regard. An expanded ECV is associated with adverse outcomes in large patient cohorts (49,55). Novel parametric mapping has been included in recent guidelines for the assessment of non-ischaemic myocardial inflammation (56), and is also named as one of 6 innovative imaging techniques for the assessment and quantification of early stages of heart failure (57). Parametric mapping techniques are expected to become the future norm for comprehensive non-invasive myocardial tissue characterisation.

### *Myocardial perfusion imaging*

Finally, contrast-enhanced myocardial perfusion imaging allows further tissue characterisation assessment in both ischaemic and non-ischaemic heart diseases.

This CMR technique uses ECG-gated fast T1-sensitive pulse sequences to capture the signal changes induced by rapid passage of an intravenous GBCA bolus (46). Images are acquired both at rest and following pharmacological stress. Coronary vasodilators are the most commonly used stress agents due to their favourable risk profile and short half-life. CMR perfusion images may be assessed 3 ways: (I) visually to identify inducible perfusion defects which may indicate obstructive coronary artery disease (CAD); (II) semi-quantitatively to assess the myocardial perfusion reserve index (MPRI), and; (III) absolute quantification of myocardial blood flow at rest and during stress, which also allows calculation of the myocardial perfusion reserve (MPR). Further technical considerations for performing stress perfusion CMR imaging may be found elsewhere (47,58).

CMR stress perfusion imaging is well-established and has been shown to outperform SPECT in detecting obstructive CAD (59-62). Recently, pixel-wise perfusion maps have been developed on selected MR vendor platforms, which allow absolute quantification of myocardial blood

flow at rest and during stress. These perfusion maps are immediately available on the scanner on-the-fly, utilising motion correction and a dual sequence approach, combining readouts suitable both for the signal dynamic ranges of the arterial input function (AIF) and myocardial tissue signals (63). These have shown promise in detecting both obstructive coronary artery disease and coronary microvascular dysfunction in a quantitative manner on these visually diagnostic perfusion maps (64).

### CMR tissue characterisation to assess cardiotoxicity

CMR is an ideal tool for the non-invasive evaluation of cardiotoxicity and serial monitoring, including cardiac structure, function and tissue characterisation. It allows identification of pathophysiological changes of cardiotoxicity, such as myocardial inflammation and oedema, the development of focal and diffuse fibrosis, and potentially early microvascular and endothelial damage, which may aid personalised treatment pathways in the management of cardiotoxicity (50).

Cardiotoxicity and LV dysfunction may be due to several potential aetiologies, with differing or overlapping pathophysiology of myocardial injury. Certain chemotherapeutics, notably anthracycline-based agents, cause direct myocellular injury, likely due to a combination of reactive oxygen species generation and inhibition of topoisomerase II beta (65). Trastuzumab (Herceptin), is a humanized monoclonal antibody targeting the HER-2 receptor which improves breast cancer survival but is known to increase the risk of cardiotoxicity and CTRCD, particularly when given in combination with anthracyclines (66). Immune checkpoint inhibitors (ICI), a new class of targeted cancer therapeutics, may cause acute myocardial inflammation, or myocarditis, with recent reports of fulminant ICI-myocarditis (67,68). The fulminant nature of this condition requires early diagnosis and prompt treatment given its malignant course. Radiation also directly damages myocardial cells via the activation of acute inflammatory cascades as well as vascular endothelial cell injury and subsequent microvascular impairment (69). These pathophysiological mechanisms have distinct biological signals which may be detected using CMR myocardial tissue characterisation techniques such as LGE imaging, and T1 or T2-mapping (56,70).

CMR LGE detects areas affected by focal myocardial scarring and fibrosis, has distinct patterns differentiating ischaemic from non-ischaemic aetiologies, and is associated

with an adverse cardiovascular prognosis in both ischaemic and non-ischaemic heart disease (45,71,72). The use of CMR LGE for the detection of cardiotoxicity have been varied, as low as 6–8% (73,74) in some studies, but approaching 100% in others (75,76). This discrepancy likely reflects significant selection bias, as studies with high rates of LGE were seen in cohorts restricted to a confirmed diagnosis of chemotherapy-related cardiotoxicity. LGE has also been seen both late and segmentally with increasing radiation dose in patients with oesophageal cancer (77), perhaps unsurprisingly, with the heart located directly within the radiation field in these cases.

Multiparametric CMR mapping techniques allow for superior non-invasive myocardial tissue characterisation compared to other imaging modalities and are able to detect subclinical disease in a broad range of myocardial pathologies (49). It is no surprise that these mapping techniques have been explored as potential early non-invasive biomarkers of cardiotoxicity. Native T1 and ECV quantitation may reflect the development of interstitial myocardial fibrosis, which has been observed to be increased in animal models of anthracycline-related cardiotoxicity (78). One recent study investigated early anthracycline cardiotoxicity by serial multiparametric CMR mapping in a porcine model; myocardial T2 values increased early following anthracycline chemotherapy, correlating with increased water content and intra-cardiomyocyte oedema, despite normal T1, ECV, and LV function (79). Interestingly in this study, withdrawal of anthracycline allowed normalisation of T2 values and regression of histological changes, while continuation led to derangement in T1 and ECV values, along with LV dysfunction and development of fibrosis (79). Although this was a porcine model with intra-coronary chemotherapy injection, it nonetheless suggests the potential of mapping techniques for identifying cardiotoxicity at an early, reversible stage.

Several clinical studies have shown elevated myocardial T1 and ECV fraction in cancer survivors previously treated with anthracyclines compared with age- and sex-matched controls (80–82). Recently, native T1 and T2 mapping have been suggested to show early CMR imaging biosignatures of CTRCD with elevations in T1 and T2 following cancer-therapy (83). Further research is required, but parametric mapping techniques show significant promise as potential early biomarkers of cardiotoxicity.

Many cancer therapies may cause clinical syndromes beyond CTRCD, including coronary artery disease and myocardial infarction. Both chemotherapy and radiotherapy

have been shown to damage the vascular endothelium (highly susceptible to radiation in particular), which predisposes to accelerated atherosclerosis or microvascular dysfunction. A linear relationship between coronary events and increasing cardiac radiation dose has been established (increase in cardiovascular risk by 7.4% per Gray mean dose to the heart), particularly in those with pre-existing cardiac risk factors or ischaemic heart disease (84). New myocardial perfusion defects have been seen 6–24 months post-cancer therapy in up to 40% of patients on nuclear SPECT imaging (85–90). As CMR stress perfusion imaging outperforms SPECT in detecting myocardial ischaemia (59–62), it may have greater utility in detecting early vascular changes following cancer therapy. Additionally, endothelial damage and microvascular dysfunction may manifest as impairments in myocardial blood flow and myocardial perfusion reserve in patients following cancer therapy; new pixel-wise perfusion maps offer a reliable and simple method for absolute quantification of myocardial blood flow during rest and stress (63,64), but have not been explored in cancer patients to-date.

### Further CMR assessments of cardiotoxicity

Although cancer-therapy-related cardiotoxicity generally focuses on CTRCD, these treatments can cause a wide variety of cardiac syndromes. CMR is also adept at evaluating valvular and pericardial disease, as well as the assessment of cardiac masses and tumours.

#### *Valvular heart disease*

Valvular heart disease is rarely seen post-chemotherapy but is a well-recognised consequence of high-dose mediastinal radiotherapy, typically with a latency period of up to 20 years. Progressive valve thickening and calcification may occur, presenting as either valvular stenosis or regurgitation (91). Aorto-mitral curtain thickening or calcification is a hallmark for previous cardiac irradiation and its extent is associated with adverse prognosis (92). Valvular abnormalities are typically imaged using transthoracic and transoesophageal echocardiography, which are gold standard for functional assessment of valvular heart disease due to their excellent temporal resolution. CMR still permits anatomical evaluation of the valve leaflets and morphology (including direct planimetry for valvular stenosis), especially when echocardiographic evaluation is suboptimal, while flow

assessments using phase contrast imaging can quantify the degree of stenosis and regurgitation (93). CMR is particularly valuable for assessing the pulmonary valve and right ventricular outflow tract, which are often not well seen on echocardiography (93).

#### *Pericardial disease*

Pericardial disease following cancer therapy is not uncommon and may also occur in the setting of tumour invasion or metastatic spread. Chemotherapy and mediastinal radiotherapy have been associated with acute pericarditis and pericardial effusions. Although acute pericarditis following radiotherapy may be self-limiting, some patients may progress to chronic pericardial inflammation or constrictive pericarditis, with thickened, fibrotic, and sometimes calcified pericardium (91). Echocardiography is first-line for initial evaluation of pericardial disease, allowing quantification of pericardial effusions, assessment of constrictive physiology, and even guiding therapeutic pericardiocentesis (26). CMR offers incremental benefit, particularly in the diagnosis of pericardial constriction. Combinations of dark-blood structural imaging, white-blood functional imaging, and real-time cine imaging during free breathing, allow assessment of the pericardium and pericardial space, as well as the haemodynamic effects of pericardial constriction or tamponade via ventricular interdependence and respirophasic septal motion (94). Myocardial tagging on CMR may provide imaging evidence of adhesion between the parietal and visceral pericardium as may be seen in constrictive pericarditis (95). Pericardial LGE is typically associated with active inflammation, while chronic constrictive pericarditis does not enhance and is associated with greater degrees of fibrosis and calcification (96). This differentiation may be helpful, as patients with active pericarditis and pericardial LGE may benefit from aggressive anti-inflammatory therapy rather than pericardiectomy (26).

#### *Cardiac masses and tumours*

The high spatial resolution afforded by CMR, along with powerful tissue characterisation techniques, makes it particularly useful for the evaluation of cardiac masses, and may help determine tissue invasion and differentiate potential aetiologies. Mass identification and localisation is initially performed with dark- and white-blood imaging sequences, followed by tissue characterisation based on

T1- and T2-weighted imaging, fat and water suppression sequences, first pass perfusion, early and late gadolinium enhancement imaging (97,98). In general, most thrombi are small, homogeneous, often associated with venous catheters, and typically hypointense on first pass perfusion, likely due to their avascular nature (98). Tumours, on the other hand, tend to be larger, display more heterogeneous tissue signal intensity, and demonstrate greater contrast uptake on first pass perfusion and LGE due to greater tumour vascularity (98). Malignant tumours, in particular, tend to be larger, cross tissue planes, and have positive LGE and first pass perfusion findings (20,98). Parametric mapping sequences have been increasingly applied to assess cardiac tumours, with several case reports demonstrating their utility (49,99-101).

### Future directions

The early detection of cardiotoxicity may afford patients considerable benefit in allowing early therapeutic intervention or modification of cytotoxic therapies. The accurate identification of which patients may be at risk of or in transition to heart failure is crucial. As outlined above, the use of novel CMR biomarkers for the detection of early cardiac injury and mechanisms underlying cardiotoxicity and cardiac dysfunction are prime targets for active research.

One such target is the myocardial energetics hypothesis, and that the failing heart is an 'engine out of fuel' (102). Briefly, cardiac energy metabolism consists of substrate utilisation, oxidative phosphorylation (and energy production), and ATP transfer and utilisation. Healthy mitochondrial function is crucial to these processes. Both chemotherapy and radiotherapy induce oxidative stress at the myocellular level, causing mitochondrial dysfunction and injury (103,104). Emerging translational MRI-based metabolic imaging techniques allow non-invasive assessment of cardiac metabolism. This presents a novel opportunity to assess myocardial energetics in patients receiving cancer therapy, given that impairments in cardiac energy metabolism typically precede any structural cardiac changes. Phosphorus magnetic resonance spectroscopy (<sup>31</sup>P-MRS) measures the myocardial phosphocreatine to adenosine triphosphate (PCr/ATP) ratio, a sensitive marker of myocardial energy status that has been shown to be impaired in patients with heart failure risk factors (i.e., obesity, diabetes) (105,106), and predict mortality in patients with dilated cardiomyopathy (107). Abnormal cardiac energy production and utilisation using <sup>31</sup>P-MRS

has been seen in animal models of anthracycline-related cardiotoxicity, with myocardial energetic changes seen to occur early and both precede and predict contractile dysfunction (108-110). Animal studies have also shown that anthracycline cardiotoxicity may be preceded by a shift from oxidative to anaerobic glucose metabolism in the heart, likely due to mitochondrial dysfunction (111). Currently the ability to perform MRS is limited to a few expert centres, but is expected to become more available as spectral quality and signal to noise ratio improves, and as further clinical utility of the technique is demonstrated.

Hyperpolarized <sup>13</sup>C magnetic resonance imaging is an emerging technology that greatly improves signal to noise ratio by transiently but dramatically increasing the signal available from a <sup>13</sup>C-labelled substrate, such as pyruvate. This may be achieved using techniques such as dynamic nuclear polarization (DNP) to artificially increase the number of molecules in a given orientation within the magnetic field and thus the polarization level (112). The enhanced signal that this technique produces allows assessment of metabolic alterations within a tissue. One of the major metabolic changes in most cancer tissues is a switch to aerobic glycolysis, known as the Warburg effect (113). Pyruvate has a central role in energy metabolism as the major product of glycolysis; it may enter the tricarboxylic acid (TCA) cycle for oxidative phosphorylation, form alanine, or, importantly, be converted to lactate by the enzyme lactate dehydrogenase (114). Overproduction of lactate is a common characteristic in most (particularly rapid-growing) cancer types, and assessment of this by hyperpolarized <sup>13</sup>C imaging may thus help characterise a tumour's metabolic phenotype *in vivo* (115). Hyperpolarized MRI has shown great potential in preclinical studies for cancer detection, grading, and monitoring therapeutic response in various disease models, such as prostate cancer, brain cancer, lymphoma, and breast cancer (116-119). Multiple clinical trials using hyperpolarized MRI for these purposes are currently underway and are highly promising.

Hyperpolarized MRI also allows unprecedented assessment of physiological and pathological changes in cardiac metabolism, and has clear potential to quantify metabolic alterations in cardiovascular disease (120). It may play an important role in understanding the metabolic changes and mechanisms of disease underlying cardiotoxicity. However, similar to MRS, hyperpolarized MRI is limited by availability, with few centres worldwide able to perform this technique at present. Nonetheless, myocardial metabolic imaging presents a new and exciting

avenue for future research, which could improve our understanding of the early cardiotoxic changes in the heart and pave the way to new cardioprotective therapies.

## Conclusions

Contemporary cancer treatments have improved long-term survival in many cancer patients. However, these therapies increase cardiac morbidity and mortality in cancer survivors via a variety of cardiotoxic mechanisms. The spectrum of disease includes subclinical cardiovascular disease to overt and fulminant cardiotoxicity and cardiac dysfunction, giving rise to the new subspecialty of cardio-oncology. CMR is increasingly utilised to provide an accurate and reproducible non-invasive assessment of cardiac structure and function, while advanced multiparametric CMR tissue characterisation techniques are gaining momentum not only in research but in clinical practice. There is a growing need for non-invasive imaging biomarkers of early cardiotoxicity, providing potential for personalised risk stratification and early therapeutic intervention, thereby reducing morbidity and mortality. Further CMR research opportunities, such as the assessment of myocardial energetics and metabolic imaging, may provide new pathophysiological insights into the disease process. Ongoing research is required to further integrate current and novel CMR techniques into future clinical guidelines for the management and surveillance of patients receiving treatment for cancer.

## Acknowledgments

VMF and MKB acknowledge support from the National Institute for Health Research (NIHR) Oxford Biomedical Research Centre at The Oxford University Hospitals NHS Foundation Trust, University of Oxford, UK.

*Funding:* VMF is supported by the British Heart Foundation, and acknowledges support from the British Heart Foundation Centre of Research Excellence in Oxford. MKB is supported by a British Heart Foundation Clinical Research Training Fellowship (FS/19/65/34692).

## Footnote

*Provenance and Peer Review:* This article was commissioned by the Guest Editors (Oliver Rider and Andrew J. Lewis) for the series “The use of advanced cardiac MRI in heart failure and cardiac hypertrophy” published in Cardiovascular Diagnosis and Therapy. The article was sent

for external peer review organized by the Guest Editors and the editorial office.

*Conflicts of Interests:* Both authors have completed the ICMJE uniform disclosure form (available at <http://dx.doi.org/10.21037/cdt-20-165>). The series “The use of advanced cardiac MRI in heart failure and cardiac hypertrophy” was commissioned by the editorial office without any funding or sponsorship. Both authors report grants from British Heart Foundation, grants from National Institute Health Research Oxford Biomedical Research Centre, during the conduct of the study. VMF reports grants from British Heart Foundation Centre of Research Excellence Oxford, outside the submitted work. The authors have no other conflicts of interest to declare.

*Ethical Statement:* The authors are accountable for all aspects of the work in ensuring that questions related to the accuracy or integrity of any part of the work are appropriately investigated and resolved.

*Open Access Statement:* This is an Open Access article distributed in accordance with the Creative Commons Attribution-NonCommercial-NoDerivs 4.0 International License (CC BY-NC-ND 4.0), which permits the non-commercial replication and distribution of the article with the strict proviso that no changes or edits are made and the original work is properly cited (including links to both the formal publication through the relevant DOI and the license). See: <https://creativecommons.org/licenses/by-nc-nd/4.0/>.

## References

1. Henry ML, Niu J, Zhang N, et al. Cardiotoxicity and Cardiac Monitoring Among Chemotherapy-Treated Breast Cancer Patients. *JACC Cardiovasc Imaging* 2018;11:1084-93.
2. Cohn KE, Stewart JR, Pajardo LF, et al. Heart disease following radiation. *Medicine (Baltimore)* 1967;46:281-98.
3. Vandercruys E, Mondelaers V, De Wolf D, et al. Late cardiotoxicity after low dose of anthracycline therapy for acute lymphoblastic leukemia in childhood. *J Cancer Surviv* 2012;6:95-101.
4. Harris EER, Correa C, Hwang WT, et al. Late Cardiac Mortality and Morbidity in Early-Stage Breast Cancer Patients After Breast-Conservation Treatment. *J Clin Oncol* 2006;24:4100-6.
5. Abdel-Qadir H, Austin PC, Lee DS, et al. A population-

- based study of cardiovascular mortality following early-stage breast cancer. *JAMA Cardiol* 2017;2:88.
6. Barac A, Murtagh G, Carver JR, et al. Cardiovascular health of patients with cancer and cancer survivors: A roadmap to the next level. *J Am Coll Cardiol* 2015;65:2739-46.
  7. Plana JC, Thavendiranathan P, Bucciarelli-Ducci C, et al. Multi-Modality Imaging in the Assessment of Cardiovascular Toxicity in the Cancer Patient. *JACC Cardiovasc Imaging* 2018;11:1173-86.
  8. Zamorano JL, Lancellotti P, Rodriguez Muñoz D, et al. 2016 ESC Position Paper on cancer treatments and cardiovascular toxicity developed under the auspices of the ESC Committee for Practice Guidelines. *Eur Heart J* 2016;37:2768-801.
  9. Felker GM, Thompson RE, Hare JM, et al. Underlying Causes and Long-Term Survival in Patients with Initially Unexplained Cardiomyopathy. *N Engl J Med* 2000;342:1077-84.
  10. Nadruz W, West E, Sengeløv M, et al. Cardiovascular phenotype and prognosis of patients with heart failure induced by cancer therapy. *Heart* 2019;105:34-41.
  11. Lyon AR. Heart failure resulting from cancer treatment: Still serious but an opportunity for prevention. *Heart* 2019;105:6-8.
  12. Liu J, Banchs J, Mousavi N, et al. Contemporary Role of Echocardiography for Clinical Decision Making in Patients During and After Cancer Therapy. *JACC Cardiovasc Imaging* 2018;11:1122-31.
  13. Chung R, Ghosh AK, Banerjee A. Cardiotoxicity: Precision medicine with imprecise definitions. *Open Heart* 2018;5:e000774.
  14. Thavendiranathan P, Grant AD, Negishi T, et al. Reproducibility of echocardiographic techniques for sequential assessment of left ventricular ejection fraction and volumes: Application to patients undergoing cancer chemotherapy. *J Am Coll Cardiol* 2013;61:77-84.
  15. Grothues F, Smith GC, Moon JC, et al. Comparison of interstudy reproducibility of cardiovascular magnetic resonance with two-dimensional echocardiography in normal subjects and in patients with heart failure or left ventricular hypertrophy. *Am J Cardiol* 2002;90:29-34.
  16. Santoro C, Arpino G, Esposito R, et al. 2D and 3D strain for detection of subclinical anthracycline cardiotoxicity in breast cancer patients: A balance with feasibility. *Eur Heart J Cardiovasc Imaging* 2017;18:930-6.
  17. Cardinale D, Colombo A, Bacchiani G, et al. Early detection of anthracycline cardiotoxicity and improvement with heart failure therapy. *Circulation* 2015;131:1981-8.
  18. Adams MJ, Hardenbergh PH, Constine LS, et al. Radiation-associated cardiovascular disease. *Crit Rev Oncol Hematol* 2003;45:55-75.
  19. Wang K, Eblan MJ, Deal AM, et al. Cardiac Toxicity After Radiotherapy for Stage III Non-Small-Cell Lung Cancer: Pooled Analysis of Dose-Escalation Trials Delivering 70 to 90 Gy. *J Clin Oncol* 2017;35:1387-94.
  20. Jordan JH, Todd RM, Vasu S, et al. Cardiovascular Magnetic Resonance in the Oncology Patient. *JACC Cardiovasc Imaging* 2018;11:1150-72.
  21. Kongbundansuk S, Hundley WG. Noninvasive imaging of cardiovascular injury related to the treatment of cancer. *JACC Cardiovasc Imaging* 2014;7:824-38.
  22. Ewer MS, Ali MK, Mackay B, et al. A comparison of cardiac biopsy grades and ejection fraction estimations in patients receiving Adriamycin. *J Clin Oncol* 1984;2:112-7.
  23. Negishi K, Negishi T, Hare JL, et al. Independent and Incremental Value of Deformation Indices for Prediction of Trastuzumab-Induced Cardiotoxicity. *J Am Soc Echocardiogr* 2013;26:493-8.
  24. Thavendiranathan P, Poulin F, Lim KD, et al. Use of Myocardial Strain Imaging by Echocardiography for the Early Detection of Cardiotoxicity in Patients During and After Cancer Chemotherapy. *J Am Coll Cardiol* 2014;63:2751-68.
  25. Narayan HK, Finkelman B, French B, et al. Detailed Echocardiographic Phenotyping in Breast Cancer Patients. *Circulation* 2017;135:1397-412.
  26. Plana JC, Galderisi M, Barac A, et al. Expert Consensus for Multimodality Imaging Evaluation of Adult Patients during and after Cancer Therapy: A Report from the American Society of Echocardiography and the European Association of Cardiovascular Imaging. *J Am Soc Echocardiogr* 2014;27:911-39.
  27. Negishi T, Thavendiranathan P, Negishi K, et al. Rationale and Design of the Strain Surveillance of Chemotherapy for Improving Cardiovascular Outcomes: The SUCCOUR Trial. *JACC Cardiovasc Imaging* 2018;11:1098-105.
  28. Farsalinos KE, Daraban AM, Ünlü S, et al. Head-to-Head Comparison of Global Longitudinal Strain Measurements among Nine Different Vendors. *J Am Soc Echocardiogr* 2015;28:1171-1181, e2.
  29. Drafts BC, Twomley KM, D'Agostino R, et al. Low to Moderate Dose Anthracycline-Based Chemotherapy Is Associated With Early Noninvasive Imaging Evidence of Subclinical Cardiovascular Disease. *JACC Cardiovasc Imaging* 2013;6:877-85.

30. Wassmuth R, Lentzsch S, Erdbruegger U, et al. Subclinical cardiotoxic effects of anthracyclines as assessed by magnetic resonance imaging—A pilot study. *Am Heart J* 2001;141:1007-13.
31. Thavendiranathan P, Wintersperger BJ, Flamm SD, et al. Cardiac MRI in the assessment of cardiac injury and toxicity from cancer chemotherapy: a systematic review. *Circ Cardiovasc Imaging* 2013;6:1080-91.
32. Armstrong GT, Plana JC, Zhang N, et al. Screening Adult Survivors of Childhood Cancer for Cardiomyopathy: Comparison of Echocardiography and Cardiac Magnetic Resonance Imaging. *J Clin Oncol* 2012;30:2876-84.
33. Schulz-Menger J, Bluemke DA, Bremerich J, et al. Standardized image interpretation and post processing in cardiovascular magnetic resonance: Society for Cardiovascular Magnetic Resonance (SCMR) board of trustees task force on standardized post processing. *J Cardiovasc Magn Reson* 2013;15:35.
34. Scatteia A, Baritussio A, Bucciarelli-Ducci C. Strain imaging using cardiac magnetic resonance. *Heart Fail Rev* 2017;22:465-76.
35. Zerhouni EA, Parish DM, Rogers WJ, et al. Human heart: Tagging with MR imaging - A new method for noninvasive assessment of myocardial motion. *Radiology* 1988;169:59-63.
36. Amzulescu MS, De Craene M, Langet H, et al. Myocardial strain imaging: review of general principles, validation, and sources of discrepancies. *Eur Heart J Cardiovasc Imaging* 2019;20:605-19.
37. Wu L, Germans T, Güçlü A, et al. Feature tracking compared with tissue tagging measurements of segmental strain by cardiovascular magnetic resonance. *J Cardiovasc Magn Reson* 2014;16:10.
38. Augustine D, Lewandowski AJ, Lazdam M, et al. Global and regional left ventricular myocardial deformation measures by magnetic resonance feature tracking in healthy volunteers: Comparison with tagging and relevance of gender. *J Cardiovasc Magn Reson* 2013;15:8.
39. Romano S, Judd RM, Kim RJ, et al. Association of Feature-Tracking Cardiac Magnetic Resonance Imaging Left Ventricular Global Longitudinal Strain With All-Cause Mortality in Patients With Reduced Left Ventricular Ejection Fraction. *Circulation* 2017;135:2313-5.
40. Jolly M-P, Jordan JH, Meléndez GC, et al. Automated assessments of circumferential strain from cine CMR correlate with LVEF declines in cancer patients early after receipt of cardio-toxic chemotherapy. *J Cardiovasc Magn Reson* 2017;19:59.
41. Nakano S, Takahashi M, Kimura F, et al. Cardiac magnetic resonance imaging-based myocardial strain study for evaluation of cardiotoxicity in breast cancer patients treated with trastuzumab: A pilot study to evaluate the feasibility of the method. *Cardiol J* 2016;23:270-80.
42. Ong G, Brezden-Masley C, Dhir V, et al. Myocardial strain imaging by cardiac magnetic resonance for detection of subclinical myocardial dysfunction in breast cancer patients receiving trastuzumab and chemotherapy. *Int J Cardiol* 2018;261:228-33.
43. Morton G, Schuster A, Jogiya R, et al. Inter-study reproducibility of cardiovascular magnetic resonance myocardial feature tracking. *J Cardiovasc Magn Reson* 2012;14:43.
44. Schuster A, Stahnke VC, Unterberg-Buchwald C, et al. Cardiovascular magnetic resonance feature-tracking assessment of myocardial mechanics: Intervendor agreement and considerations regarding reproducibility. *Clin Radiol* 2015;70:989-98.
45. Mahrholdt H, Wagner A, Judd RM, et al. Delayed enhancement cardiovascular magnetic resonance assessment of non-ischaemic cardiomyopathies. *Eur Heart J* 2005;26:1461-74.
46. Ferrari V. The EACVI Textbook of Cardiovascular Magnetic Resonance. In: Lombardi M, Plein S, Petersen S, et al., editors. *The EACVI Textbook of Cardiovascular Magnetic Resonance*. Oxford University Press; 2018.
47. Kramer CM, Barkhausen J, Flamm SD, et al. Standardized cardiovascular magnetic resonance (CMR) protocols 2013 update. *J Cardiovasc Magn Reson* 2013;15:91.
48. Ferreira VM, Piechnik SK, Dall'Armellina E, et al. Non-contrast T1-mapping detects acute myocardial edema with high diagnostic accuracy: a comparison to T2-weighted cardiovascular magnetic resonance. *J Cardiovasc Magn Reson* 2012;14:42.
49. Messroghli DR, Moon JC, Ferreira VM, et al. Clinical recommendations for cardiovascular magnetic resonance mapping of T1, T2, T2\* and extracellular volume: A consensus statement by the Society for Cardiovascular Magnetic Resonance (SCMR) endorsed by the European Association for Cardiovascular Imagi. *J Cardiovasc Magn Reson* 2017;19:75.
50. Karamitsos TD, Arvanitaki A, Karvounis H, et al. Myocardial Tissue Characterization and Fibrosis by Imaging. *JACC Cardiovasc Imaging* 2020. [Epub ahead of print].
51. Ntusi NAB, Piechnik SK, Francis JM, et al. Subclinical

- myocardial inflammation and diffuse fibrosis are common in systemic sclerosis - a clinical study using myocardial T1-mapping and extracellular volume quantification. *J Cardiovasc Magn Reson* 2014;16:21.
52. Ferreira VM, Piechnik SK, Dall'Armellina E, et al. T1 Mapping for the Diagnosis of Acute Myocarditis Using CMR: Comparison to T2-Weighted and Late Gadolinium Enhanced Imaging. *JACC Cardiovasc Imaging* 2013;6:1048-58.
  53. Ntusi NAB, Piechnik SK, Francis JM, et al. Diffuse Myocardial Fibrosis and Inflammation in Rheumatoid Arthritis. *JACC Cardiovasc Imaging* 2015;8:526-36.
  54. Ferreira VM, Marcelino M, Piechnik SK, et al. Pheochromocytoma is characterized by catecholamine-mediated myocarditis, focal and diffuse myocardial fibrosis, and myocardial dysfunction. *J Am Coll Cardiol* 2016;67:2364-74.
  55. Treibel TA, Fridman Y, Bering P, et al. Extracellular Volume Associates With Outcomes More Strongly Than Native or Post-Contrast Myocardial T1. *JACC Cardiovasc Imaging* 2020;13:44-54.
  56. Ferreira VM, Schulz-Menger J, Holmvang G, et al. Cardiovascular Magnetic Resonance in Nonischemic Myocardial Inflammation: Expert Recommendations. *J Am Coll Cardiol* 2018;72:3158-76.
  57. Čelutkienė J, Plymen CM, Flachskampf FA, et al. Innovative imaging methods in heart failure: a shifting paradigm in cardiac assessment. Position statement on behalf of the Heart Failure Association of the European Society of Cardiology. *Eur J Heart Fail* 2018;20:1615-33.
  58. Biglands JD, Radjenovic A, Ridgway JP. Cardiovascular magnetic resonance physics for clinicians: part II. *J Cardiovasc Magn Reson* 2012;14:66.
  59. Greenwood JP, Maredia N, Younger JF, et al. Cardiovascular magnetic resonance and single-photon emission computed tomography for diagnosis of coronary heart disease (CE-MARC): A prospective trial. *Lancet* 2012;379:453-60.
  60. Schwitter J, Wacker CM, Wilke N, et al. MR-IMPACT II: Magnetic resonance imaging for myocardial perfusion assessment in coronary artery disease trial: Perfusion-cardiac magnetic resonance vs. single-photon emission computed tomography for the detection of coronary artery disease: A comparative. *Eur Heart J* 2013;34:775-81.
  61. Nagel E, Greenwood JP, McCann GP, et al. Magnetic resonance perfusion or fractional flow reserve in coronary disease. *N Engl J Med* 2019;380:2418-28.
  62. Kwong RY, Ge Y, Steel K, et al. Cardiac Magnetic Resonance Stress Perfusion Imaging for Evaluation of Patients With Chest Pain. *J Am Coll Cardiol* 2019;74:1741-55.
  63. Kellman P, Hansen MS, Nielles-Vallespin S, et al. Myocardial perfusion cardiovascular magnetic resonance: optimized dual sequence and reconstruction for quantification. *J Cardiovasc Magn Reson* 2017;19:43.
  64. Kotecha T, Martinez-Naharro A, Boldrini M, et al. Automated Pixel-Wise Quantitative Myocardial Perfusion Mapping by CMR to Detect Obstructive Coronary Artery Disease and Coronary Microvascular Dysfunction: Validation Against Invasive Coronary Physiology. *JACC Cardiovasc Imaging* 2019;12:1958-69.
  65. Sawyer DB. Anthracyclines and heart failure. *N Engl J Med* 2013;368:1154-6.
  66. Slamon DJ, Leyland-Jones B, Shak S, et al. Use of Chemotherapy plus a Monoclonal Antibody against HER2 for Metastatic Breast Cancer That Overexpresses HER2. *N Engl J Med* 2001;344:783-92.
  67. Johnson DB, Balko JM, Compton ML, et al. Fulminant myocarditis with combination immune checkpoint blockade. *N Engl J Med* 2016;375:1749-55.
  68. Mahmood SS, Fradley MG, Cohen J V., et al. Myocarditis in Patients Treated With Immune Checkpoint Inhibitors. *J Am Coll Cardiol* 2018;71:1755-64.
  69. Rahimi CC, McGale K, Ferreira P, et al. Effects of Radiation Therapy on the Cardiovascular System. In: Yeh E, editor. *Cancer and the Heart*. MD Anderson, Texas; 2012.
  70. Friedrich MG, Sechtem U, Schulz-Menger J, et al. Cardiovascular Magnetic Resonance in Myocarditis: A JACC White Paper. *J Am Coll Cardiol* 2009;53:1475-87.
  71. Shanbhag SM, Greve AM, Aspelund T, et al. Prevalence and prognosis of ischaemic and non-ischaemic myocardial fibrosis in older adults. *Eur Heart J* 2019;40:529-38.
  72. Becker MAJ, Cornel JH, van de Ven PM, et al. The Prognostic Value of Late Gadolinium-Enhanced Cardiac Magnetic Resonance Imaging in Nonischemic Dilated Cardiomyopathy: A Review and Meta-Analysis. *JACC Cardiovasc Imaging* 2018;11:1274-84.
  73. Neilan TG, Coelho-Filho OR, Pena-Herrera D, et al. Left ventricular mass in patients with a cardiomyopathy after treatment with anthracyclines. *Am J Cardiol* 2012;110:1679-86.
  74. Lawley C, Wainwright C, Segelov E, et al. Pilot study evaluating the role of cardiac magnetic resonance imaging in monitoring adjuvant trastuzumab therapy for breast cancer. *Asia Pac J Clin Oncol* 2012;8:95-100.

75. Fallah-Rad N, Lytwyn M, Fang T, et al. Delayed contrast enhancement cardiac magnetic resonance imaging in trastuzumab induced cardiomyopathy. *J Cardiovasc Magn Reson* 2008;10:5.
76. Wadhwa D, Fallah-Rad N, Grenier D, et al. Trastuzumab mediated cardiotoxicity in the setting of adjuvant chemotherapy for breast cancer: A retrospective study. *Breast Cancer Res Treat* 2009;117:357-64.
77. Umezawa R, Ota H, Takanami K, et al. MRI findings of radiation-induced myocardial damage in patients with oesophageal cancer. *Clin Radiol* 2014;69:1273-9.
78. Farhad H, Staziaki P V, Addison D, et al. Characterization of the changes in cardiac structure and function in mice treated with anthracyclines using serial cardiac magnetic resonance imaging. *Circ Cardiovasc Imaging* 2016;9:e003584.
79. Galán-Arriola C, Lobo M, Vílchez-Tschischke JP, et al. Serial Magnetic Resonance Imaging to Identify Early Stages of Anthracycline-Induced Cardiotoxicity. *J Am Coll Cardiol* 2019;73:779-91.
80. Jordan JH, Vasu S, Morgan TM, et al. Anthracycline-Associated T1 Mapping Characteristics Are Elevated Independent of the Presence of Cardiovascular Comorbidities in Cancer Survivors. *Circ Cardiovasc Imaging* 2016;9:e004325.
81. Neilan TG, Coelho-Filho OR, Shah R V, et al. Myocardial Extracellular Volume by Cardiac Magnetic Resonance Imaging in Patients Treated With Anthracycline-Based Chemotherapy. *Am J Cardiol* 2013;111:717-22.
82. Meléndez GC, Jordan JH, D'Agostino RB, et al. Progressive 3-Month Increase in LV Myocardial ECV After Anthracycline-Based Chemotherapy. *JACC Cardiovasc Imaging* 2017;10:708-9.
83. Haslbauer JD, Lindner S, Valbuena-Lopez S, et al. CMR imaging biosignature of cardiac involvement due to cancer-related treatment by T1 and T2 mapping. *Int J Cardiol* 2019;275:179-86.
84. Darby SC, Ewertz M, McGale P, et al. Risk of ischemic heart disease in women after radiotherapy for breast cancer. *N Engl J Med* 2013;368:987-98.
85. Marks LB, Yu X, Prosnitz RG, et al. The incidence and functional consequences of RT-associated cardiac perfusion defects. *Int J Radiat Oncol Biol Phys* 2005;63:214-23.
86. Gyenes G, Fornander T, Carlens P, et al. Morbidity of ischemic heart disease in early breast cancer 15-20 years after adjuvant radiotherapy. *Int J Radiat Oncol Biol Phys* 1994;28:1235-41.
87. Gyenes G, Fornander T, Carlens P, et al. Myocardial damage in breast cancer patients treated with adjuvant radiotherapy: A prospective study. *Int J Radiat Oncol Biol Phys* 1996;36:899-905.
88. Seddon B, Cook A, Gothard L, et al. Detection of defects in myocardial perfusion imaging in patients with early breast cancer treated with radiotherapy. *Radiother Oncol* 2002;64:53-63.
89. Tzonevska A, Tzvetkov K, Parvanova V, et al. <sup>99m</sup>Tc-MIBI myocardial perfusion scintigraphy for assessment of myocardial damage after radiotherapy in patients with breast cancer. *J BUON* 2006;11:505-9.
90. Sioka C, Exarchopoulos T, Tasiou I, et al. Myocardial perfusion imaging with (99 m)Tc-tetrofosmin SPECT in breast cancer patients that received postoperative radiotherapy: a case-control study. *Radiat Oncol* 2011;6:151.
91. Desai MY, Windecker S, Lancellotti P, et al. Prevention, Diagnosis, and Management of Radiation-Associated Cardiac Disease. *J Am Coll Cardiol*. 2019;74:905-27.
92. Desai MY, Wu W, Masri A, et al. Increased Aorto-Mitral Curtain Thickness Independently Predicts Mortality in Patients With Radiation-Associated Cardiac Disease Undergoing Cardiac Surgery. *Ann Thorac Surg* 2014;97:1348-55.
93. Myerson SG. Heart valve disease: Investigation by cardiovascular magnetic resonance. *J Cardiovasc Magn Reson* 2012;14:7.
94. White CS. MR evaluation of the pericardium and cardiac malignancies. *Magn Reson Imaging Clin N Am* 1996;4:237-51.
95. Kojima S, Yamada N, Goto Y. Diagnosis of Constrictive Pericarditis by Tagged Cine Magnetic Resonance Imaging. *N Engl J Med* 1999;341:373-4.
96. Zurick AO, Bolen MA, Kwon DH, et al. Pericardial Delayed Hyperenhancement With CMR Imaging in Patients With Constrictive Pericarditis Undergoing Surgical Pericardiectomy. *JACC Cardiovasc Imaging* 2011;4:1180-91.
97. Fussen S, De Boeck BWL, Zellweger MJ, et al. Cardiovascular magnetic resonance imaging for diagnosis and clinical management of suspected cardiac masses and tumours. *Eur Heart J* 2011;32:1551-60.
98. Pazos-López P, Pozo E, Siqueira ME, et al. Value of CMR for the Differential Diagnosis of Cardiac Masses. *JACC Cardiovasc Imaging* 2014;7:896-905.
99. Ferreira VM, Holloway CJ, Piechnik SK, et al. Is it really fat? Ask a T1-map. *Eur Heart J Cardiovasc Imaging* 2013;14:1060.

100. Burrage M, Dahiya A, Ng ACT, et al. Multimodality imaging of a rare case of cardiac lipomatosis. *Eur Heart J Cardiovasc Imaging* 2017;18:115.
101. Watson WD, Ferreira VM, Sayeed R, et al. Serial Cardiac Magnetic Resonance of an Evolving Subacute Pericardial Hematoma. *Circ Cardiovasc Imaging* 2019;12:e009753.
102. Neubauer S. The failing heart - An engine out of fuel. *N Engl J Med* 2007;356:1140-51.
103. Boerma M, Sridharan V, Mao XW, et al. Effects of ionizing radiation on the heart. *Mutat Res* 2016;770:319-27.
104. Montaigne D, Hurt C, Neviere R. Mitochondria death/survival signaling pathways in cardiotoxicity induced by anthracyclines and anticancer-targeted therapies. *Biochem Res Int* 2012;2012:951539.
105. Levelt E, Rodgers CT, Clarke WT, et al. Cardiac energetics, oxygenation, and perfusion during increased workload in patients with type 2 diabetes mellitus. *Eur Heart J* 2016;37:3461-9.
106. Rider OJ, Francis JM, Ali MK, et al. Effects of catecholamine stress on diastolic function and myocardial energetics in obesity. *Circulation* 2012;125:1511-9.
107. Neubauer S, Horn M, Cramer M, et al. Myocardial Phosphocreatine-to-ATP Ratio Is a Predictor of Mortality in Patients With Dilated Cardiomyopathy. *Circulation* 1997;96:2190-6.
108. Dekker T, Kirkels JH, Ruigrok TJJ, et al. Chronic cardiotoxicity of adriamycin studied in a rat model by 31P NMR. *NMR Biomed* 1991;4:16-24.
109. Bittner V, Reeves RC, Digerness SB, et al. 31P NMR spectroscopy in chronic adriamycin cardiotoxicity. *Magn Reson Med* 1991;17:69-81.
110. Maslov MY, Chacko VP, Hirsch GA, et al. Reduced in vivo high-energy phosphates precede adriamycin-induced cardiac dysfunction. *Am J Physiol Heart Circ Physiol* 2010;299:H332-7.
111. Timm KN, Perera C, Ball V, et al. Mitochondrial dysfunction in a rat model of doxorubicin-induced heart failure assessed by hyperpolarized 13C MRS. In: *Proceedings of the International Society for Magnetic Resonance in Medicine*. 2019. p. 27:078.
112. Rider OJ, Tyler DJ. Clinical Implications of Cardiac Hyperpolarized Magnetic Resonance Imaging. *J Cardiovasc Magn Reson* 2013;15:93.
113. Warburg O. On the origin of cancer cells. *Science* 1956;123:309-14.
114. von Morze C, Merritt ME. Cancer in the crosshairs: targeting cancer metabolism with hyperpolarized carbon-13 MRI technology. *NMR Biomed* 2019;32:e3937.
115. Golman K, Zandt RI, Lerche M, et al. Metabolic imaging by hyperpolarized 13C magnetic resonance imaging for in vivo tumor diagnosis. *Cancer Res* 2006;66:10855-60.
116. Albers MJ, Bok R, Chen AP, et al. Hyperpolarized 13C lactate, pyruvate, and alanine: Noninvasive biomarkers for prostate cancer detection and grading. *Cancer Res* 2008;68:8607-15.
117. Park I, Larson PEZ, Gordon JW, et al. Development of methods and feasibility of using hyperpolarized carbon-13 imaging data for evaluating brain metabolism in patient studies. *Magn Reson Med* 2018;80:864-73.
118. Day SE, Kettunen MI, Gallagher FA, et al. Detecting tumor response to treatment using hyperpolarized 13C magnetic resonance imaging and spectroscopy. *Nat Med* 2007;13:1382-7.
119. Witney TH, Kettunen MI, Hu DE, et al. Detecting treatment response in a model of human breast adenocarcinoma using hyperpolarised 1- 13 C pyruvate and 1,4- 13 C 2 fumarate. *Br J Cancer* 2010;103:1400-6.
120. Rider OJ, Apps A, Miller JJ, et al. Non-Invasive In Vivo Assessment of Cardiac Metabolism in the Healthy and Diabetic Human Heart Using Hyperpolarized 13 C MRI. *Circ Res* 2020;126:725-36.

**Cite this article as:** Burrage MK, Ferreira VM. The use of cardiovascular magnetic resonance as an early non-invasive biomarker for cardiotoxicity in cardio-oncology. *Cardiovasc Diagn Ther* 2020;10(3):610-624. doi: 10.21037/cdt-20-165